Chapter 1

Neutrino oscillations

1.1 Physics motivations

Although the standard model describes very successfully particle physics in terms of three families, to date two of these component are still under investigation. In particular, one of these, the t quark is the subject of intensive search at Fermilab, whereas the ν_τ is unobserved though extensively searches in various laboratories are under way. So far only inference on its existence are carried on. The table 1.1 shows the elementary particles of matter, namely quarks that make up strongly interacting matter, and the weakly interacting leptons. The mass of these elementary matter particles are also indicated.

Results from LEP experiments show that there are only three species of light neutrino. By measuring the rate of Z^o decay into neutral particles, LEP has determined the effective number of neutrino species: $N_\nu = 2.985 \pm 0.023$.

Quarks	$\begin{pmatrix} +2/3 \\ -1/3 \end{pmatrix} \begin{pmatrix} u \\ d \end{pmatrix} \begin{pmatrix} 5MeV \\ 8MeV \end{pmatrix}$	$\begin{pmatrix} c \\ s \end{pmatrix} \begin{pmatrix} 1.5GeV \\ 0.15GeV \end{pmatrix}$	$\begin{pmatrix} t \\ b \end{pmatrix} \begin{pmatrix} 170GeV \\ 5Gev \end{pmatrix}$
Leptons	$\begin{pmatrix} 0 \\ -1 \end{pmatrix} \quad \begin{pmatrix} \nu_e \\ e^- \end{pmatrix} \begin{pmatrix} \leq 7eV \\ 0.5MeV \end{pmatrix}$	$\begin{pmatrix} \nu_\mu \\ \mu^- \end{pmatrix} \begin{pmatrix} \leq 0.27MeV \\ 0.1GeV \end{pmatrix}$	$\begin{pmatrix} \nu_\tau \\ \tau \end{pmatrix} \begin{pmatrix} \leq 31MeV \\ 1,78GeV \end{pmatrix}$

Table 1.1:

It should be noted that there are only upper limits on the neutrino masses, and the search on the possible existence of massive neutrinos could be an important item of the modern physics.

If neutrino indeed has a finite mass then many new opportunities would be open both for theoretical and for experimental physics. For example, massive neutrino is the most natural candidate for hot dark matter particles.

The quark mixing is very well known. It is very likely that neutrinos are also mixed. Neutrino mass and mixing make possible the phenomenon of neutrino oscillations [1, 2]. In the simplified case in which oscillations are assumed to occur between two neutrino species, the probability of an initial ν_i, of energy E_ν being equal to ν_j at a distance L is

$$P(\nu_i \rightarrow \nu_j) = \sin^2 2\theta \sin^2[\frac{1.27\Delta m^2 L}{E_\nu}] \tag{1.1}$$

where Δm^2 in eV^2, L in Km and E_ν in GeV.

For massive neutrinos the see saw mechanism relates the mass:

$$m_{\nu_\tau} : m_{\nu_\mu} : m_{\nu_e} = m_\tau^2 : m_\mu^2 : m_e^2$$

This means that a measurement of m_{ν_τ} implies indications of m_{ν_μ} and m_{ν_e}.

Concerning the ν_τ, τ pair, the following questions are still open:

- direct observation of ν_τ,
- possible existence of ν_τ mass,
- possible mass mixing between ν_τ and ν_e, ν_μ.

The present experimental scenario is presented in this chapter, together with the oscillation limits obtained so far. Hints on neutrino mass, even if based on weak and controversial results come from accelerator, atmospheric and solar neutrino experiments.

1.2 Atmospheric neutrinos

1.2.1 Introduction

Atmospheric neutrinos originate mainly from the decays of π's, K's and μ's produced in cosmic-ray-induced air showers. From the decay chains (1.2)

one expects the ratio of the number of ν_μ's and $\overline{\nu}_\mu$'s to ν_e's and $\overline{\nu}_e$'s to be approximately equal to two at low energy (1$\sim$2 GeV).

$$\pi, K \rightarrow \mu\nu_\mu$$
$$\mu \rightarrow e\nu_\mu\nu_e \qquad (1.2)$$

Neutrino interactions (which represent the background in nucleon decay searches) have been recorded in the large nucleon decay detectors. Atmospheric neutrino interactions are identified in different energy range:
i) by means of their interactions within a massive target detector. The detector can be a water Čerenkov (IMB [3], Kamiokande [4]) or tracking calorimeter apparatus (NUSEX [5], Soudan 2 [6], Frejus [7]). Neutrino interactions are then classified as fully or partially contained, depending on whether all interaction products are contained within the detector fiducial volume. The interaction rate is proportional to the detector mass.
ii) by means of the muons produced by ν_μ interactions in the rock surrounding the detector, with the produced muon either completely traversing or stopping in the detector. In this case, the interaction rate is proportional to the apparatus area. The calculated energies of atmospheric neutrinos giving rise to contained events and to the observed upward throughgoing/stopping muons are shown in Fig. 1.1 for a generic experiment.

Assuming a simple two-flavors neutrino oscillation in vacuum, the probability that a ν_μ remains in the same state is given by $1 - P(\nu_i \rightarrow \nu_j)$, where $P(\nu_i \rightarrow \nu_j)$ is the oscillation probability 1.1.
Different types of measurements probe different parts of the neutrino spectrum; using the energy distribution of Fig. 1.1 and the production distance for the neutrinos the ratio E_ν/L can be estimated. This sets the scale for the region in the Δm^2 parameter accessible to each data sample in the expression for the ν oscillation probability (1.1). The $sin^2 2\theta$ parameter is mainly limited by the statistics.

1.2.2 Contained events

The water Čerenkov experiments Kamiokande [4] and IMB [3] separated charged current (CC) muon from CC electron interactions and found that the ratio of muons to electrons was smaller than expected.

Neutrino interactions are identified *i*) using the shape of the Čerenkov ring on the phototubes on the wall of the apparatus [8]; *ii*) through the

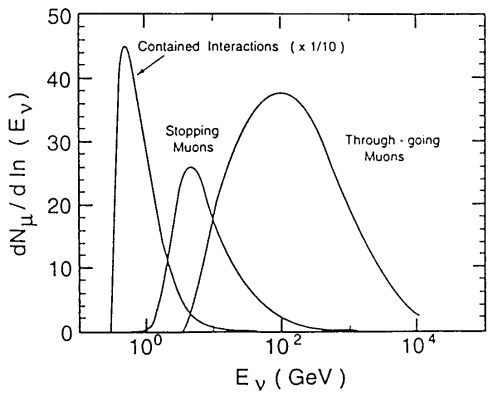

Figure 1.1: Approximate energy distribution of atmospheric neutrinos giving rise to (partially) contained events and (stopping) throughgoing muons in an underground generic experiment.

recognition of the muon decay in a time window several microseconds after an event classified as contained [3, 9].

Also tracking calorimetric experiments (NUSEX [5], Frejus [7], and Soudan 2 [6]) have analyzed their data, searching for contained interactions and tried also to separate ν_μ from ν_e CC interactions. All experiments express their results in terms of the ratio between $R^{obs} = (\frac{\nu_\mu}{\nu_e})^{obs}$ from measured CC interaction events and $R^{MC} = (\frac{\nu_\mu}{\nu_e})^{MC}$ from a Montecarlo simulation.

Although the single ratios may be affected by rather large theoretical and systematic uncertainties, in the ratio:

$$R = \frac{(\frac{\nu_\mu+\overline{\nu}_\mu}{\nu_e+\overline{\nu}_e})^{obs}}{(\frac{\nu_\mu+\overline{\nu}_\mu}{\nu_e+\overline{\nu}_e})^{MC}} \tag{1.3}$$

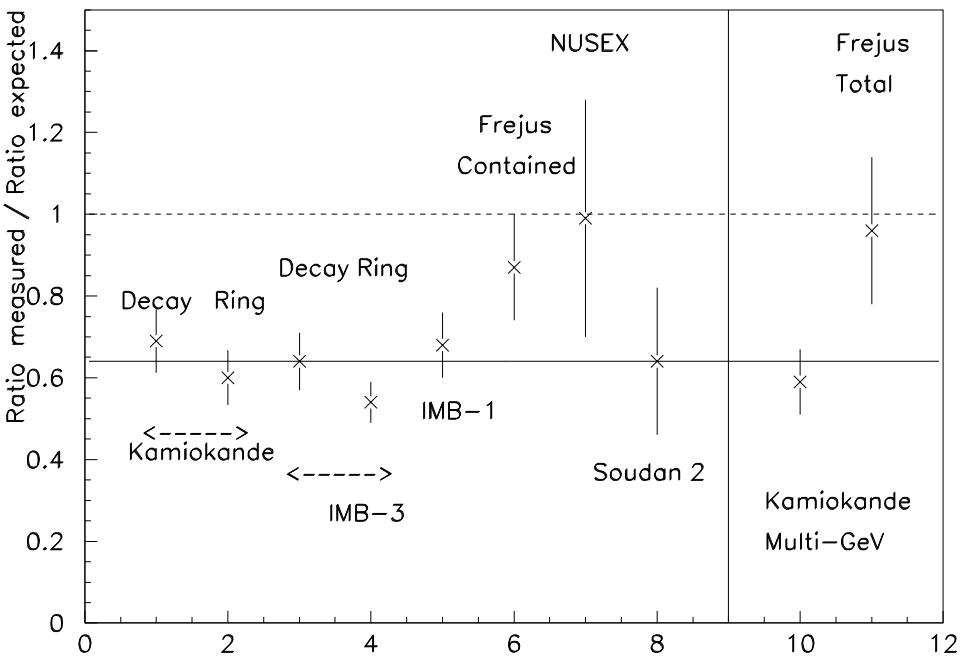

Figure 1.2: The ratio R (see text) measured in water Čerenkov detectors (Kamiokande, IMB) and in calorimetric experiments (NUSEX, Frejus, and Soudan 2).

most theoretical uncertainties (as well as systematics properties of each particular detector) effectively cancel. In Fig. 1.2 a summary of the results on atmospheric ν contained and partially contained events is shown.

Most experimental results on contained atmospheric neutrino events are consistent with a $30-40\%$ deficit of ν_μ events. Such a deficit could be the result of either $\nu_\mu \leftrightarrow \nu_\tau$ or $\nu_\mu \leftrightarrow \nu_e$ oscillations or both , or of some effect(s) other than neutrino oscillations.

The solution in terms of $(\nu_\mu \leftrightarrow \nu_e)$ oscillation is inconsistent with the solar neutrino results, which require Δm^2 of the order of $10^{-5} eV^2$ if interpreted in terms of oscillations, as discussed in the next paragraph. Moreover, the $\nu_\mu \leftrightarrow \nu_\tau$ interpretation of the small R ratio for contained events is favourite by the preliminary results [10] on the measurement of the intensity of muons at the atmospheric depth where both μ and ν are produced. This makes

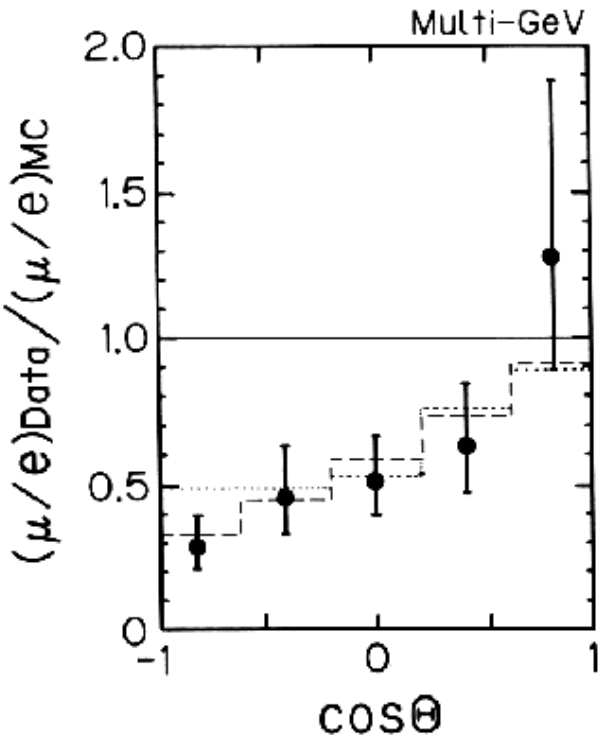

Figure 1.3: Zenith angle distribution of the ratio R where both the fully contained and the partially contained Kamiokande events are included. Best fits curves for the neutrino oscillation hypothesis with parameters in the text are also shown. This angular dependance agrees with a model in which the path length for downward going ν_μ ($L \sim 10 - 20\ Km$) is too short for oscillations, while the upward going ν_μ flux ($L \sim 12000\ Km$) is reduced by more than a factor two.

the hypothesis of $\nu_\mu \leftrightarrow \nu_\tau$ the favoured one for the interpretation of the contained atmospheric neutrino data. In particular, the allowed regions in the oscillation parameter space from the Kamiokande data are:
$\Delta m^2 > 4 \times 10^{-3}\ eV^2$ and $sin^2 2\theta > 0.3$ for $\nu_\mu \leftrightarrow \nu_e$ and $\Delta m^2 > 1 \times 10^{-3}\ eV^2$ and $sin^2 2\theta > 0.4$ for $\nu_\mu \leftrightarrow \nu_\tau$ oscillations.

1.2.3 Partially contained events

A different analysis has been performed by the Kamiokande group [11] in the so-called multi-GeV energy range. These events are (i) fully-contained events with E_{vis} larger than 1.33 GeV, and (ii) partially-contained events which have their interaction vertex in the fiducial volume and at least one

Experiment	Observed	Calculated	
		"high"	"low"
IMB	0.47 ± 0.02	-	0.455
KAM	2.04 ± 0.14	2.36	2.18
Baksan	161	162	142
MACRO	$74 \pm 9 \pm 8$	101 ± 15	-

Table 1.2: Upward muon fluxes. The units for Kamiokande (KAM) are $10^{-13} cm^{-2} s^{-1} sr^{-1}$; for IMB, events per day; for Baksan and MACRO, the total number of observed events.

visible track exiting from the inner-detector. These data constitute a completely independent data sample from the contained events data quoted above. The estimated mean energy of neutrinos is 5 GeV for the fully-contained e-like events, 2.5 GeV for the fully-contained μ-like events, and 9 GeV for the partially- contained μ-like events. The estimated ratio R is $R = 0.57^{+0.08}_{-0.07}(stat) \pm 0.07(syst)$ based on the Bartol neutrino flux [12].

For this data sample it is possible to extract the zenith distribution of the events, which is claimed to be inconsistent with the no-oscillation hypothesis (Fig. 1.3). Assuming oscillations, the best fit to the data correspond to oscillation parameters:
$\nu_\mu \leftrightarrow \nu_e$ $(\Delta m^2 = 1.8 \times 10^{-2}\ eV^2, \Delta sin^2 2\theta = 1.0)$ dashes, and $\nu_\mu \leftrightarrow \nu_\tau$ $(\Delta m^2 = 1.6 \times 10^{-2} eV^2, \Delta sin^2 2\theta = 1.0)$ dots.

1.2.4 Upward going and stopping μ

The flux of muon neutrinos in the energy region from a few GeV up to hundreds of GeV can be inferred from measurements of upgoing muons in underground detectors (see Fig. 1.1). Measurements of the flux of upgoing muons with sufficiently large energies to penetrate through detectors have been made by the Baksan [13], Kamiokande [14], IMB [15] and MACRO [16] detectors with no apparent discrepancy with expectations from calculation. These measurements, which are summarized in Table 1.2, exclude part of the allowed region from Kamiokande contained events data.
However, it was pointed out [1] that the wide range of the $(\Delta m^2, sin^2 2\theta)$ parameter space for the ν_μ disappearance in Fig. 1.4 (the 90% $C.L.$ excluded regions shown in this figure came from [18],[15],[7],[19],[20], [21]) excluded by

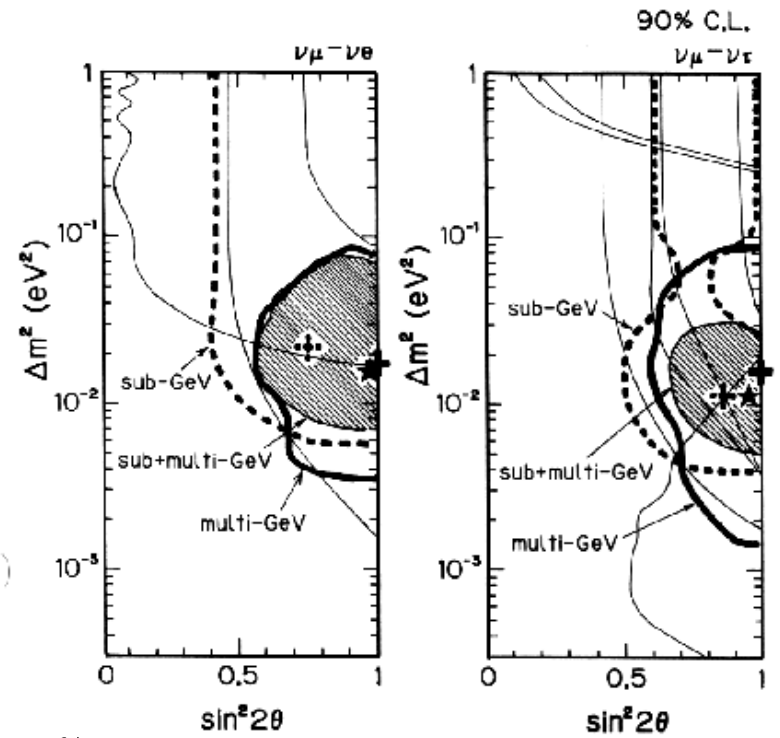

Figure 1.4: 90% C.L. allowed neutrino-oscillation parameters as obtained from the multi-GeV data (thick curves). 90% C.L. allowed regions as obtained from the updated sub-GeV data are also shown by thick-dotted curves. The allowed regions as obtained by combining the sub- and multi-GeV data are also shown (shaded region). The best-fit values are also shown by dash-crosses (sub-GeV data), full-crosses (multi-GeV data) and stars (sub- and multi-GeV data combined).

analysis of the absolute flux of upward throughgoing muons can be overestimated due to the present uncertainties on the assumed neutrino flux, nucleon structure function and muon propagation in the rock.

Most theoretical uncertainties cancel when the ratio between upward going stopping muons ($UGS\mu$) over throughgoing muons ($UG\mu$) is calculated. At present, waiting for Kamiokande and MACRO results, only the IMB collaboration published this value, where the statistical error on the $UGS\mu$ fraction is somewhat larger than the uncertainty in the theoretical calculation. The exclusion region partially overlaps with allowed region for $\nu_\mu \leftrightarrow \nu_\tau$ oscillations obtained with partially contained events. In this measurement a possible background is constituted by upward going pions induced by pho-

	DATA	SSM	DATA/SSM
GALLEX (SNU)	$79 \pm 10 \pm 6$	132	0.598 ± 0.088
SAGE (SNU)	$69 \pm 10^{+5}_{-7}$	132	0.532 ± 0.088
Kamiokande			
$(10^6 cm^{-2} s^{-1})$	$2.75^{+0.20}_{-018} \pm 0.41$	5.69	0.484 ± 0.079
Homestake (SNU)	$2.55 \pm 0.17 \pm 0.18$	8.0	0.319 ± 0.031

Table 1.3: The solar-neutrino data of 1995 compared with the SSM prediction.

tonuclear interaction of atmospheric muons in the rock. The pion can mimic a low energy muon, stopping in the detector. Some evidences of this effect in underground detector was seen by the MACRO [22] experiment.

1.3 The Solar neutrino problem

To complete the general overview on the non-accelerator neutrino oscillation problem, we briefly mention the results concerning Solar Neutrinos. All four solar-neutrino experiment [23], [24], [25], [26]report a deficit in the measured fluxes. The data, as reported in 1995 [27] , are listed in Table 1.3 and compared with calculations of Bachall and Pinnsoneault [27] for the Standard Solar Model (SSM).

At the present stage of knowledge of the physics of the Sun and of the nuclear cross sections relevant for neutrino production in the Sun, a nuclear/astrophysical solution to the solar neutrino problem seems strongly disfavoured, while the MSW solution [30] can explain the results of all four neutrino experiments. This model implies ν_e disappearance with parameters $\Delta m^2 \sim 10^{-5} eV^2$ and $sin^2(2\theta) \sim 0.01$ or, alternatively, $sin^2(2\theta) \sim 0.8$. In case of vacuum oscillations interpretation Δm^2 is of the order of $10^{-10} eV^2$.

1.4 Neutrino Oscillation at Accelerators

High energy accelerators provide ν_μ beams as a result of K, π and μ decay, allowing the study of $\nu_\mu \rightarrow \nu_e$ and $\nu_\mu \rightarrow \nu_\tau$ channels. The expression of the oscillation probability is given by 1.1. therefore the range of Δm^2 values which can be explored in neutrino oscillation experiment depends on the

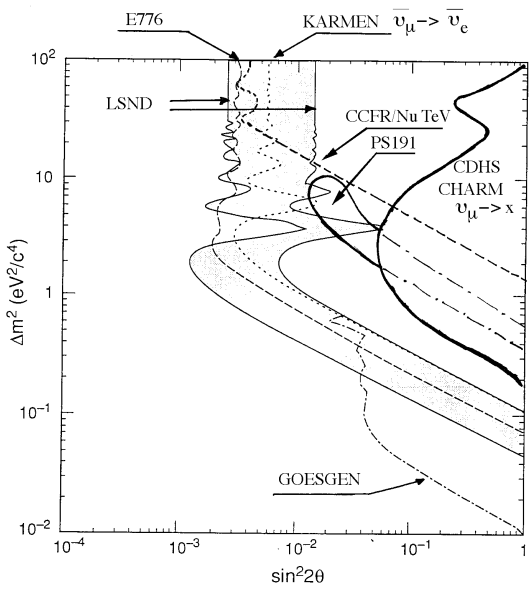

Figure 1.5: The exclusion plot of $\nu_\mu \rightarrow \nu_e$ oscillations at accelerators.

distance between source and detector, as well as on the energy of the neutrino beam. So far accelerator experiments are capable of investigating very small mixing angles and relative high values of Δm^2 ($\geq 1\ eV^2$).

1.4.1 Searches for $\nu_\mu \rightarrow \nu_e$ Oscillations

Search for appearance of $\nu_\mu \rightarrow \nu_e$ oscillation have been carried out in many experiments [32]. The type of neutrino beam used, the mode of detecting oscillations and their results are listed in table 1.4.

In Fig. 1.5 the exclusion plots obtained by these experiments are shown.

Of particular interest is the unconventional neutrino beam at LAMPF (Los Alamos Mesons Physics facility). The neutrino source consists of an equal mixture of ν_μ, $\bar{\nu_\mu}$, ν_e, arising from the decay of stopped π^+ and μ^+, which are produced by 780 MeV proton beam dump. Observation of ν_e, $\bar{\nu}_e$ production above that expected from conventional processes may be inter-

FEATURES OF $\nu_\mu \to \nu_e, \overline{\nu}_\mu \to \overline{\nu}_e$ EXPERIMENTS

Experiments	beams	Detector	Reactions	Oscill. Limits
Lampf 84 1984	Los Alamos $\overline{\nu}_\mu$	Plastic scintillator and Flashtubes, 14 tons	$\overline{\nu}_e + p \to e^+ + n$ $35 < E_e < 53$ Mev	$\Delta m^2 < 0.49$ eV^2 for max. mix. $\sin^2 2\vartheta < 0.028$ for < 2eV^2
Lampf E645 E764 1988	Los Alamos ν_μ, $\overline{\nu}_\mu$	Liquid scintillator planes Proportional drift tubes Gadolinium layers	$\overline{\nu}_e + p \to e^+ + n$ $+ (n, \gamma)$ in Gd	$\Delta m^2 < 0.11$ eV^2 for max. mix. $\sin^2 2\theta < 0.014$ for large Δm^2
BNL 734 1985	Brookhaven ν_μ	Liquid scintillator planes Proportional drift chamber	$\nu_\mu + n \to \mu^- + p$ $\nu_e + n \to e^- + p$	$\Delta m^2 < 0.43$ eV^2 for max. mix. $\sin^2 2\theta < 3.4.10^{-3}$ large Δm^2
PS 191 1986	CERN PS ν_μ	Calorimeter flash-tubes Iron plates	$\nu_\mu + n \to \mu^- + p$ $\nu_e + n \to e^- + p$	Excess of electrons at: $\Delta m^2 \approx$ (5-10) eV^2 $\sin^2 2\theta \approx$ (0.02-0.04)
BNL 816 1987	Brookhaven ν_μ	PS 191 moved at BNL	$\nu_\mu + n \to \mu^- + p$ $\nu_e + n \to e^- + p$	No excess seen
BNL E776 1987	Brookhaven ν_μ	Calorimeter	$\nu_\mu + n \to \mu^- + p$ $\nu_e + n \to e^- + p$	$\Delta m^2 < 8.8.10^{-2}$ eV^2 for max. mix. $\sin^2 2\theta < 3.5.10^{-3}$ for large Δm^2
CDHS CHARM 1984-86	CERN PS ν_μ	Two experiments at 130 m and 885 m. 100, 600 tons	$\nu_\mu + n \to \mu^- + p$ $\nu_e + n \to e^- + p$ + appearance	$0.26 < \Delta m^2 < 96$ eV^2 for max. mix. and $\sin^2 2\theta < 0.053$ for $\Delta m^2 \approx 2.5$ eV^2
BEBC 1986	CERN PS ν_μ	Bubble chamber 14 tons	$\nu_\mu + n \to \mu^- + p$ $\nu_e + n \to e^- + p$	$\Delta m^2 < 0.09$ eV^2 for max. mix. $\sin^2 2\theta < 0.013$ for $\Delta m^2 = 2.2$ eV^2
FNAL 15 ft 1981	Fermilab ν_μ	Bubble chamber	$\nu_\mu + n \to \mu^- + p$ $\nu_e + n \to e^- + p$	$\Delta m^2 < 0.6$ eV^2 for max. mix. $\sin^2 2\theta < 6.10^{-3}$ for large Δm^2
SKAT 1988	Serpukov ν_μ	Bubble chamber	$\nu_\mu + n \to \mu^- + p$ $\nu_e + n \to e^- + p$	$\Delta m^2 > 1.3$ eV^2 for max. mix. $\sin^2 2\theta < 2.5.10^{-3}$ for $\Delta m^2 = 60$ eV^2
CCFR 1984	Fermilab ν_μ	two detector 715 and 1116m.	$\nu_\mu + n \to \mu^- + p$ $\nu_e + n \to e^- + p$ + disappearance	$\Delta m^2 < 15$ eV^2 or $\Delta m^2 > 10^3$eV^2 for max. mix., $\sin^2 2\theta < 0.02$ for $\Delta m^2 \approx 100$eV^2
CCFR/NuTeV running	Fermilab ν_μ	390 fiducial tons: Fe, scintillator, drift chambers	$\nu_\mu + n \to \mu^- + p$ $\nu_e + n \to e^- + p$	$\Delta m^2 < 2$ eV^2 for max. mix. $\sin^2 2\theta < 4.10^{-3}$ for large Δm^2
LSND Lampf running	Los Alamos ν_μ, $\overline{\nu}_\mu$, ν_e	200 tons of mineral oil (Cerenkov light) plus scintillator (energy) 1220 PMT's	$\overline{\nu}_e + p \to e^+ + n$ $+ (n, \gamma)$ in Gd $\nu_e + {}^{12}C \to e^- X$	excess of $e^+ \gamma$ at $\Delta m^2 \approx 6$ eV^2 $\Delta m^2 < 0.07$eV^2 for max. mix., $\sin^2 2\theta < 6.10^{-3}$ for large Δm^2
KARMEN running	ISIS Rutherford ν_μ, $\overline{\nu}_\mu$, ν_e	56 tons high resolution liquid scintillation calorimeter and gadolinium	$\overline{\nu}_e + p \to e^+ + n$ $+ (n, \gamma)$ in Gd $\nu_e + {}^{12}C \to e^- X$ $X \to {}^{12}C + e^+ \nu_e$ delayed	$\nu_\mu \to \nu_e$: $\Delta m^2 < 0.2$ for max. mix., $\sin^2 2\theta < 5.10^{-2}$ for large Δm^2. $\overline{\nu}_\mu \to \overline{\nu}_e$: $\Delta m^2 < 0.08$ for max.mix., $\sin^2 2\theta < 6.10$-3 for large Δm^2. time anomaly in π^+ decay

Table 1.4:

preted as evidence for $\bar{\nu}_\mu \to \bar{\nu}_e$, $\nu_\mu \to \nu_e$ oscillations.

The most recent Liquid Scintillator Neutrino Detector (LSND) [33], is based on 200 tons mineral oil Cherenkov counter. The presence of ν_e and $\bar{\nu}_e$ in the beam is detected via the reaction

$$\nu_e + C \to e^- + N$$

giving an electron, and

$$\bar{\nu}_e + p \to e^+ + n$$

giving a positron in the energy range 36–60 MeV. The positron signal is followed by 2.2 MeV gamma ray due to the absorption of the recoil neutron by the free protons of the scintillator. Electron and positron produced in this reaction emit scintillation and Cherenkov light which are recorded by 1220 photomultipliers.

In Fig. 1.5 are also reported the exclusion plots dor LSND, KARMEN and CCFR experiments [33].

Even if LSND experiment claims a weak signal for $\bar{\nu}_\mu \to \bar{\nu}_e$ oscillation, no other experiment shows clear signatures in the region $\Delta m^2 \geq 0.1$ eV^2, $\sin^2 2\theta \geq 2 \cdot 10^{-3}$. Therefore further investigations are needed in next years.

1.4.2 Searches for $\nu_\mu \to \nu_\tau$ Oscillations

In the past several searches for ν_τ appearance have been performed at Fermilab using nuclear emulsion. Due to the very good spatial resolution (μm) such detectors are able to see decays of short lived particles produced in neutrino interactions. It was, therefore, possible to look for the evidence of tau lepton production. In table 1.5 are reported the main detector and relative results obtained so far, together with present or planned experiments [31, 32].

Many efforts are also done to achieve good statistics and τ identification capability. In order to push down the limits on the mixing angles a clear recognition of ν_τ, observing the finite path of the τ lepton before its decay, in a fine active target is needed. Then the use of emulsion and/or scintillating fibers could be one possible approach. This technique is followed by two experiments CHORUS [34] and P803 [35] respectively at CERN and FERMILAB. Emulsion stacks comprising both fixed bulk emulsion and changeable sheet are followed by scintillating fiber trackers. Magnet, tracking chambers, calorimeter and muon detector complete the experiments.

A complementary method, based on kinematical analysis criteria, is used by the NOMAD[36] experiment at CERN. The principle is to distinguish $\nu_\tau +$

FEATURES OF $\nu_\mu \to \nu_\tau$ EXPERIMENTS

Experiments	beams	Detector	Reactions	Oscill. Limits
E 531 1986	Fermilab ν_μ	Emulsion target	$\nu_\mu + N \to \tau + X$	Δm^2 <1 eV^2 for max. mix. $sin^2 2\theta$ <4.10^{-3} for large Δm^2
E 564 1986	Fermilab ν_μ	Emulsions in bubble chamber	$\nu_\mu + N \to \tau + X$	Δm^2 <4 eV^2 for max. mix. $sin^2 2\theta$ <8.10^{-2} for large Δm^2
E 803 approved	Fermilab ν_μ	Emulsions, fiber trackers, drift chambers, calorimeter, muon detector, magnet, 0.5t	$\nu_\mu + N \to \tau + X$	Δm^2 <0.2 eV^2 for max. mix. $sin^2 2\theta$ <2.10^{-5} for large Δm^2
Chorus running	Cern ν_μ	Emulsions, fiber trackers, streamer tubes, calorimeter, muon detector, magnet, 0.8t	$\nu_\mu + N \to \tau + X$	Δm^2 <1 eV^2 for max. mix. $sin^2 2\theta$ <2.10^{-4} for large Δm^2
Nomad running	Cern ν_μ	Drift chambers, TRD, calorimeter, muon detector, magnet, 1.2 t	$\nu_\mu + N \to \tau + X$	Δm^2 <1 eV^2 for max. mix. $sin^2 2\theta$ <2.10^{-4} for large Δm^2

Table 1.5:

$N \to \tau + X$ from background using purely kinematical cuts such as missing $p_\perp$, missing energy and angular correlations. This requires an apparatus with very good energy, momentum, and angular resolution. The target consists of 150 drift chambers inside a magnet. The detector includes also transition radiation detector, lead glass, and a muon detector. The ν_μ beam is generated by 450 GeV proton extracted from SPS machine and impinged on a beryllium target. The detector are approximately 800 m away from the target after the decay tunnel.

The exclusion plots of $\nu_\mu \to \nu_\tau$ relative to CHORUS and NOMAD, compared to that relative to P803 are shown in Fig. 1.6.

1.5 Long baseline experiments

As described in section 1.2 atmospheric neutrino experiments performed in underground laboratories show an anomaly in the contained charged current neutrino interaction, interpreted as a possible signal for neutrino oscillation. To increase the sensitivity of accelerator neutrino experiments down and beyond the region indicated by atmospheric neutrino data ($\Delta m^2 \sim 10^{-3}$) the

Laboratory	Beams	Detector	Reactions	Distance	Oscillation limits
FNAL MINOS proposal	ν_μ 120 GeV proton 5.10^{13} p/1.9 sec	Streamer tubes, iron and magnetic field, 1.5 T. 10 Kt 480000 channels + near detector	$\nu_\mu N \to \mu X$ $\nu_e N \to eX$	730 Km.	$\nu_\mu \to \nu_\tau$: $\Delta m^2 < 10^{-3}$ eV^2 $sin^2 2\theta < 3.10^{-2}$ 2 years $\nu_\mu \to \nu_e$: $\Delta m^2 < 6.10^{-4}$eV^2 $sin^2 2\theta < 6.10^{-2}$ 2 years
FNAL SOUDAN 2 existing + upgrading	ν_μ 120 GeV proton 5.10^{13} p/1.9 sec	Calorimeter steel and drift tubes toroid 840 tons near detector 50 t.	$\nu_\mu N \to \mu X$ $\nu_e N \to eX$	730 Km.	$\nu_\mu \to \nu_\tau$: $\Delta m^2 < 2.10^{-3}$ eV^2 $sin^2 2\theta < 8.10^{-2}$ 2 years $\nu_\mu \to \nu_e$: $\Delta m^2 < 10^{-3}$eV^2 $sin^2 2\theta < 2.10^{-2}$ 2 years
UNK BAIKAL proposal	ν_μ 600 GeV	Underwater Cerenkov detector	$\nu_\mu N \to \mu X$ disappearance	4200 Km.	$\Delta m^2 < 10^{-3}$ eV^2 $sin^2 2\theta < 2.10^{-2}$
KEK Superkamioka under costruction	ν_μ 12 GeV 4.10^{12}p/2.5 sec	Water Cerenkov detector	$\nu_\mu N \to \mu X$ $\nu_e N \to eX$	250 Km.	$\nu_\mu \to \nu_\tau$: $\Delta m^2 < 2.10^{-3}$ eV^2 $sin^2 2\theta < 0.2$ $\nu_\mu \to \nu_e$: $\Delta m^2 < 3.10^{-3}$eV^2 $sin^2 2\theta < 0.1$
ICARUS approved	ν_μ 450 GeV 2.10^{13}p/7.2 sec	TPC liquid Argon 600 tons	$\nu_\mu N \to \mu X$ $\nu_e N \to eX$		$\nu_\mu \to \nu_\tau$: $\Delta m^2 < 6.10^{-3}$ eV^2 $sin^2 2\theta < 10^{-1}$ $\nu_\mu \to \nu_e$: $\Delta m^2 < 3.10^{-3}$eV^2 $sin^2 2\theta < 10^{-2}$
CERN - GS ICARUS proposal	ν_μ 450 GeV 2.10^{13}p/7.2 sec	TPC liquid Argon 4.7 Ktons	$\nu_\mu N \to \mu X$ $\nu_e N \to eX$	730 Km.	$\nu_\mu \to \nu_\tau$: $\Delta m^2 < 2.10^{-3}$ eV^2 $sin^2 2\theta < 3.10^{-2}$ 2.5 years $\nu_\mu \to \nu_e$: $\Delta m^2 < 10^{-3}$eV^2 $sin^2 2\theta < 10^{-2}$ 2.5 years
CERN - GS RICH proposal	ν_μ 450 GeV 2.10^{13}p/7.2 sec	Rich detectors 14-18 Kt H_2O as target, 350000 channels	$\nu_\mu N \to \mu X$ $\nu_e N \to eX$	730 Km.	
CERN - GS NOE proposal	ν_μ 450 GeV 2.10^{13}p/7.2 sec	Calorimeter 6Kt scintillating fibers streamer tubes or RPC Iron ore	$\nu_\mu N \to \mu X$ $\nu_e N \to eX$	730 Km.	$\nu_\mu \to \nu_\tau$: $\Delta m^2 < 2.10^{-3}$ eV^2 $sin^2 2\theta < 3.10^{-2}$ 4 years $\nu_\mu \to \nu_e$: $\Delta m^2 < 10^{-3}$eV^2 $sin^2 2\theta < 10^{-2}$ 4 years

Table 1.6:

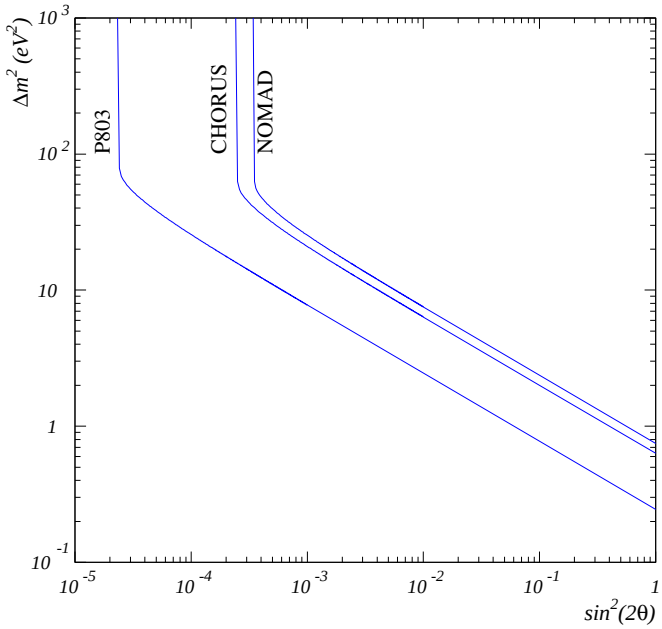

Figure 1.6: The exclusion plot of $\nu_\mu \to \nu_\tau$ oscillations at accelerators.

baseline must be extended outside the limits of the accelerator and reactor laboratory.

Now there are serious proposal to detect neutrinos at long distance from reactor ($\sim$ Km) and from high energy accelerators ($\sim$ hundreds of kilometers) with devoted underground detectors. The sensitivity achievable is down to $10^{-2} - 10^{-3}$ in Δm^2. This long baseline experiments represent a complementary approach to the short baseline experiments which are studying smaller $sin^2 2\theta$ values.

Long baseline neutrino beam projects are under discussion in various Laboratories in the world [37, 38, 39, 4].

Constraints determined by the energy and luminosity of present accelerator determine the limits in the oscillation space parameters achievable when the detector is placed far from the neutrino source. In table 1.6 are shown experiments planned or under construction. Concerning reactor experiment the CHOOZ detector has been funded and is today in advanced state of construction [41]. The sensitivity for disappearance of $\bar{\nu}_e$ will be down to 10^{-3} eV^2. Reactor long baseline experiments are shown in table 1.7 [41, 42]. Due to the kinematics, the main disadvantage is that the appearance of $\bar{\nu}_e \to \bar{\nu}_\mu$ and $\bar{\nu}_e \to \bar{\nu}_\tau$ cannot be visible.

LONG BASELINE REACTOR EXPERIMENTS

Experiment	**neutrino target mass**	**reactor distance**	Δm^2 **(min.)**
Krasnoyarsk project	600 kg	230 m	0.01
San Onofre project	12000 kg	680 m	2.10^{-3}
Chooz running	4800 kg	1025 m	10^{-3}
Perry future	1000 ton	12.9 km	10^{-4}

Table 1.7:

Bibliography

[1] Z.Maki et al., *Prog. Theo. Phys. 28* (1962) 1870

[2] B.Pontecorvo, *Zh. Eksp. Theor. Fiz. 33* (1957) 549

[3] R. Becker-Szendy et al. (IMB Coll.) - Phys. Rev. D 46,3720(1992)

[4] K.S.Hirata et al. (Kamiokande II Coll.) - Phys. Lett. B 280,146(1992)

[5] M.Aglietta et al.(NUSEX Coll.), Europhys. Lett. 8,611(1989)

[6] W.A.Mann et al. (Soudan 2 Coll.) - Phys. Lett. B291,200 (1992)

[7] Ch. Berger et al. (Frejus Coll.) - Phys. Lett. B 245,305(1990)

[8] M.Takita, Doctor Thesis, University of Tokio, ICR Report 186-89-3 (1989)

[9] Kamiokande presentation at Neutrino '94, Eilat, Israel, 1994 (to be published in the proceedings)

[10] M.Circella et al. in Proc 23rd Int. Cosmic Ray Conf., Calgary, 1993, Vol.4, p.503

[11] Y.Fukuda et al. - Phys. Lett. B 335, 237(1994)

[12] T.Gaisser et al., Ph. Rev D39(1989)3532

[13] M.M.Boliev et al. (Baksan Coll.), in Proc. 3rd Int. Workshop on Neutrino Telescopes, Venice, 1991, edited by M. Baldo Ceolin, p. 235

[14] M.Mori et al. - Phys. Lett. B270,89(1991)

[15] R.Becker-Szendy et al. - Phys. Rev. Lett. 69,1010(1992)

[16] S.Ahlen et al. (MACRO Coll.) - Phys.Lett. B357(1995)481

[17] W.Frati et al. - Phys. Rev. D48, 1140(1993)

[18] Y.Oyama et al. - Phys. Rev. D39(1989)1481

[19] K.Gabathuler et al. - Phys. Lett. B 138(1984)449

[20] F.Dydak et al. - Phys.Lett.B134(1984)281

[21] F.Bergsma et al. - Phys.Lett. B142(1984) 103

[22] M.Spurio, private communication

[23] P.Anselman et al. (GALLEX Coll.), Phys. Lett. 327B,377 (1994)

[24] J.N.Abdurashitov et al (SAGE Coll.), Talk at 27th Int. Conf. on High Energy Physics, Glasgow 20-27 July 1994

[25] K.Inoue, Talk at XXX Rencontre de Moriond, March 12-18, 1995

[26] B.T.Cleveland et al. (Homestake), Nuclear Phys. B (Proc. Suppl.) 39,47, (1995)

[27] J.N.Bahcall and M.Pinnsoneault, Rev.Mod. Phys. 64, 885, (1992)

[28] J.N.Bahcall, Neutrino Astrophysics, Cambridge Univ. Press, Cambridge, 1989

[29] S. Turck-Chieze, W. Dappen, E. Fossat, J.Provost,E.Schatzmann and D.Vignaud, Phys. Rep. 230,57,(1993)

[30] S.P.Mikheyev and A.Yu.Smirnov, Yadern. Fiz., 42, 1441,(1985);L.Wolfenstein, Phys, Rev.D17,2369(1978)

[31] Boehm F., Vogel P.- Physics of Massive Neutrinos - Cambridge-University Press

[32] Oberaurer L. and Feilitzsch - Neutrinos oscillation review. Rep. Prog. Phys. 55 (1992) 1093-1163.

[33] CCFR/NuTeV, LSND, KARMEN collaborations - EPS Conference, July 1995

[34] CHORUS - CERN - PPE/93 - 131 (1993) and CERN - SPSC/90 - 42 SPSC, P 254.

[35] P 803 - Proposal for a short baseline experiment at Fermilab, October 1990

[36] NOMAD - CERN - SPSLC/91- 21SPSC P261 (1991) and CERN - SPSLC/93 - 31 SPSLC M525 (1993).

[37] P-875 A long baseline Neutrino Oscillation Experiment at Fermilab, February 1995.

[38] P-822 Proposal for a long baseline Neutrino Oscillation Experiment using the SOUDAN Neutrino Detector.

[39] UNK-BAIKAL, KEK-SUPERKAMIOKANDE, ICARUS, RICH detector, NOE proposals presented at Long Baseline Neutrino Workshop. Gran Sasso 9/11/1995

[40] Cavanna F. The Cern-Gran Sasso Long Baseline Neutrino-Beam Project, CERN-PPE/95-133 (1995).

[41] R.I. Steinberg. Proc. 5th Workshop on Neutrino Telescopes ed. Milla Baldo Ceolin, 209, Padova, 1993.

[42] Y.Declais. Proc. 6th Workshop on Neutrino Telescopes ed. Milla Baldo Ceolin, 455 Padova, 1993.